Charmless B decays: Dalitz

Marianna Fontana on behalf of the LHCb collaboration

Max-Planck-Institut für Kernphysik, Heidelberg

Beauty conference 2014

Edinburgh, 14 - 18 July 2014

Outline

- Physics motivation
- Experimental results
  - CPV in the $B^{\pm} \to h^{+}h^{-}h^{\pm}$decays New
  - CPV in the $B^{\pm} \to p\bar{p}h^{\pm}$decays New

  where $h = \pi/K$
- Conclusions

Physics motivation

- B charmless decays provide an interesting environment to search for CP violation
- They can have contributions by tree and penguin diagrams

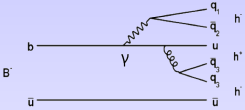

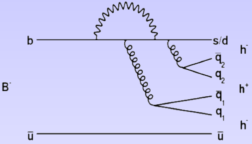

- Interference between these topologies can give rise to direct CP violation: contribution of at least two amplitudes with different weak and strong phases
- Three-body charmless decays allow to study interfering strong phases
- The strong phase can come from different sources:
  - Short distance processes
  - Long distance processes with hadron-hadron interactions in the final state:
    - final state $KK \leftrightarrow \pi\pi$ rescattering
    - interference between intermediate states

$B^{\pm} \to h^{+}h^{-}h^{\pm}$ decays

Direct CPV in $B^{\pm} \to h^+ h^- h^{\pm}$

LHCb-PAPER-2014-044 in preparation

- **Motivation**:
  - Evidence of direct CPV in $B^{\pm} \to h^+ h^- h^{\pm}$ decays ($1 fb^{-1}$) [PRL 111 (2013) 101810] [PRL 112 (2014) 011801]
  - Source of the strong phase difference not well understood
- **Analysis** uses 3 fb^{-1} of data recorded by LHCb in 2011 and 2012:
  - Selection strategy improved w.r.t. the previous analysis
  - Use of a Boosted Decision Tree to reduce the combinatorial background
  - New particle identification discriminating variables
- **Measurements**:
  - Inclusive CP asymmetry
  - CP asymmetry in the phase space

Inclusive CP asymmetry [LHCb-PAPER-2014-044 Preliminary]

Measurement of the raw CP asymmetry from simultaneous mass fit to B^{+} and B^{-} candidate:

$$\mathcal{A}_{raw} = \frac{N_{B^-} - N_{B^+}}{N_{B^-} + N_{B^+}}$$

$B^{-} \to K^{-}\pi^{+}\pi^{-}$ $B^{+} \to K^{+}\pi^{+}\pi^{-}$

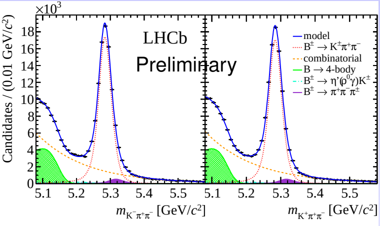

$B^{-} \to K^{-}K^{+}K^{-}$ $B^{+} \to K^{+}K^{+}K^{-}$

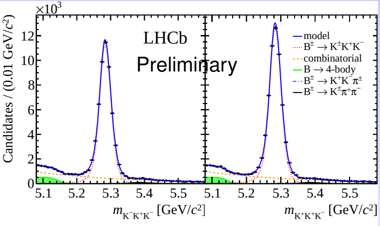

$B^{-} \to \pi^{-}\pi^{+}\pi^{-}$ $B^{+} \to \pi^{+}\pi^{+}\pi^{-}$

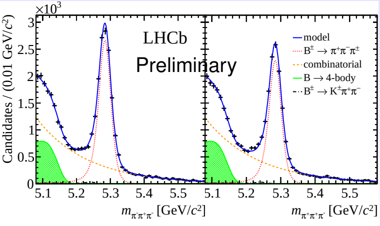

$B^{-} \to K^{-}K^{+}\pi^{-}$ $B^{+} \to K^{+}K^{+}\pi^{-}$

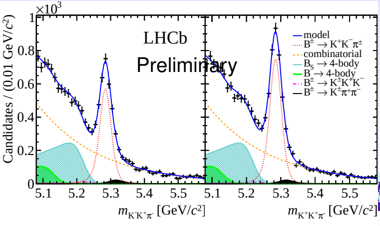

Inclusive CP asymmetry [LHCb-PAPER-2014-044 Preliminary]

NEW

- The raw asymmetry has to be corrected for detector acceptance and the B-meson production asymmetry:

$$\mathcal{A}_{raw} \approx \mathcal{A}_{CP} + \mathcal{A}_{P} + \mathcal{A}_{D}^{h'}$$ small asymmetries

- Decays divided into two categories depending on the flavour of the unpaired hadron:

$B^{\pm} \to h^+ h^- K^{\pm}$ $\qquad \mathcal{A}_{CP} = \mathcal{A}_{raw} - \mathcal{A}_P(B^{\pm}) - \mathcal{A}_D(K^{\pm})$

$B^{\pm} \to h^+ h^- \pi^{\pm}$ $\qquad \mathcal{A}_{CP} = \mathcal{A}_{raw} - \mathcal{A}_P(B^{\pm}) - \mathcal{A}_D(\pi^{\pm})$

  - $\mathcal{A}_P(B)$ from $B \to J/\psi(\mu\mu)K$ studies and using $\mathcal{A}_D(K) = (-0.126 \pm 0.018)\%$ [PRL 108 (2012) 201601]
  - $\mathcal{A}_D(\pi) = (0.00 \pm 0.25)\%$ from studies of prompt D^+ decays [PLB 713 (2012) 186]

- Acceptance correction to take into account non uniformity of efficiencies and raw asymmetries in the phase space

Preliminary

$$\mathcal{A}_{CP}(B^{\pm} \to K^{\pm}\pi^{+}\pi^{-}) = +0.025 \pm 0.004\,(\text{stat}) \pm 0.004\,(\text{syst}) \pm 0.007(J/\psi\, K^{\pm}) \quad 2.8\sigma$$
$$\mathcal{A}_{CP}(B^{\pm} \to K^{\pm}K^{+}K^{-}) = -0.036 \pm 0.004\,(\text{stat}) \pm 0.002\,(\text{syst}) \pm 0.007(J/\psi\, K^{\pm}) \quad 4.3\sigma$$
$$\mathcal{A}_{CP}(B^{\pm} \to \pi^{\pm}\pi^{+}\pi^{-}) = +0.058 \pm 0.008\,(\text{stat}) \pm 0.009\,(\text{syst}) \pm 0.007(J/\psi\, K^{\pm}) \quad 4.2\sigma$$
$$\mathcal{A}_{CP}(B^{\pm} \to \pi^{\pm}K^{+}K^{-}) = -0.123 \pm 0.017\,(\text{stat}) \pm 0.012\,(\text{syst}) \pm 0.007(J/\psi\, K^{\pm}) \quad 5.6\sigma$$

Dalitz plots [LHCb-PAPER-2014-044 Preliminary]

Dalitz plots in the signal region with bkg: $\pm 34\ MeV/c^2$ (*hhh* and *hhK*), $\pm 17\ MeV/c^2$ (πKK)

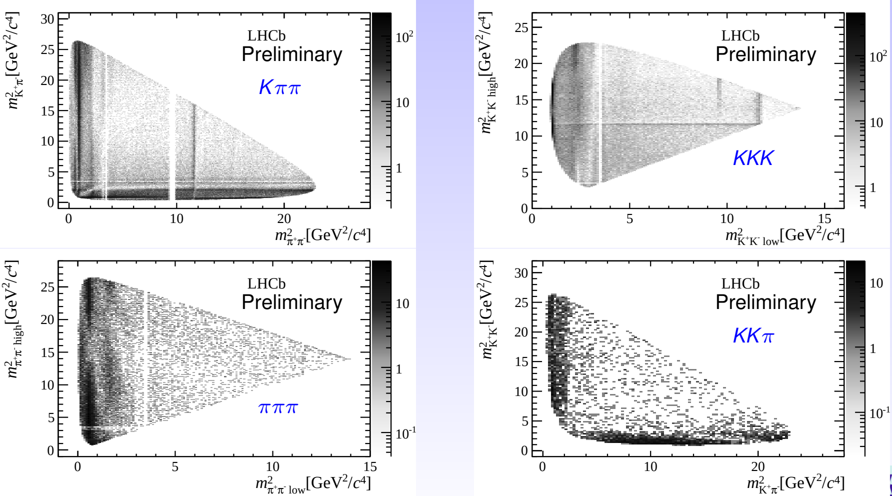

Dalitz plots [LHCb-PAPER-2014-044 Preliminary]

NEW

Dalitz plots in the signal region with bkg: $\pm 34\ MeV/c^2$ (hhh and hhK), $\pm 17\ MeV/c^2$ (πKK)

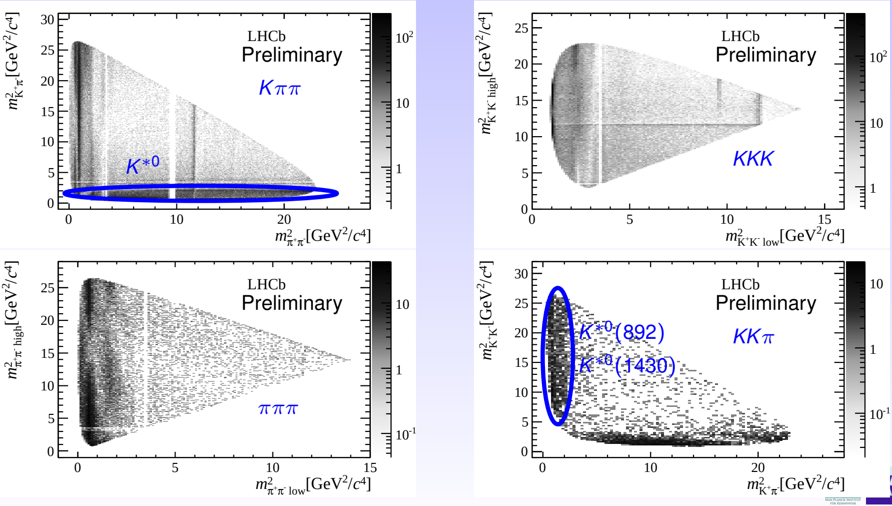

Dalitz plots [LHCb-PAPER-2014-044 Preliminary]

NEW

Dalitz plots in the signal region with bkg: $\pm 34\ MeV/c^2$ (hhh and hhK), $\pm 17\ MeV/c^2$ (πKK)

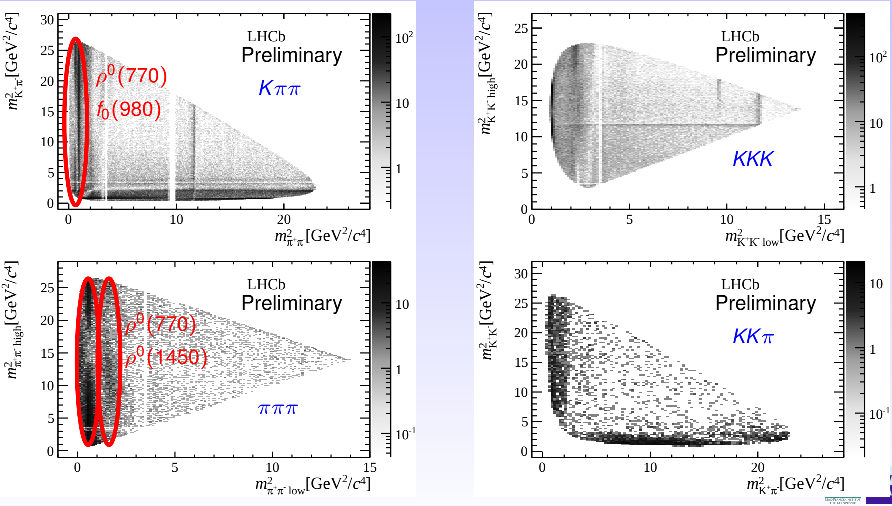

Dalitz plots [LHCb-PAPER-2014-044 Preliminary]

Dalitz plots in the signal region with bkg: ± 34 MeV/c^2 (hhh and hhK), ± 17 MeV/c^2 (πKK)

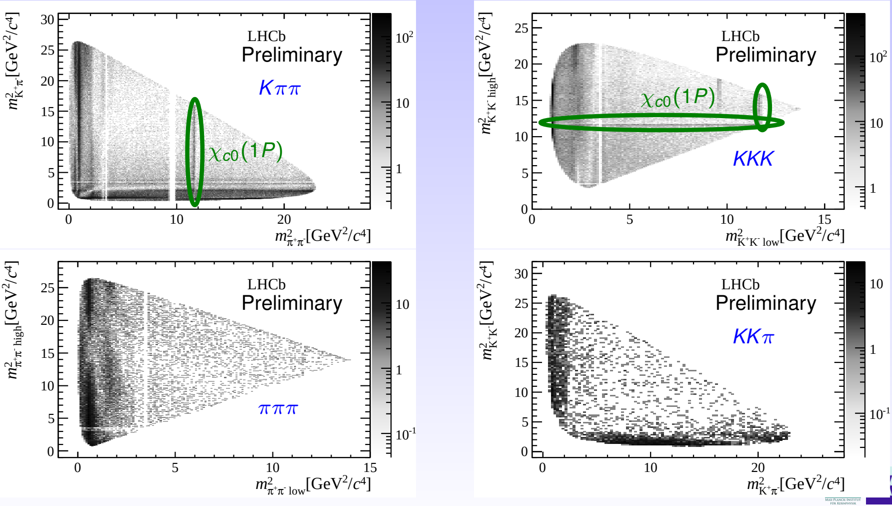

Dalitz plots [LHCb-PAPER-2014-044 Preliminary]

Dalitz plots in the signal region with bkg: ± 34 MeV/c^2 (hhh and hhK), ± 17 MeV/c^2 (πKK)

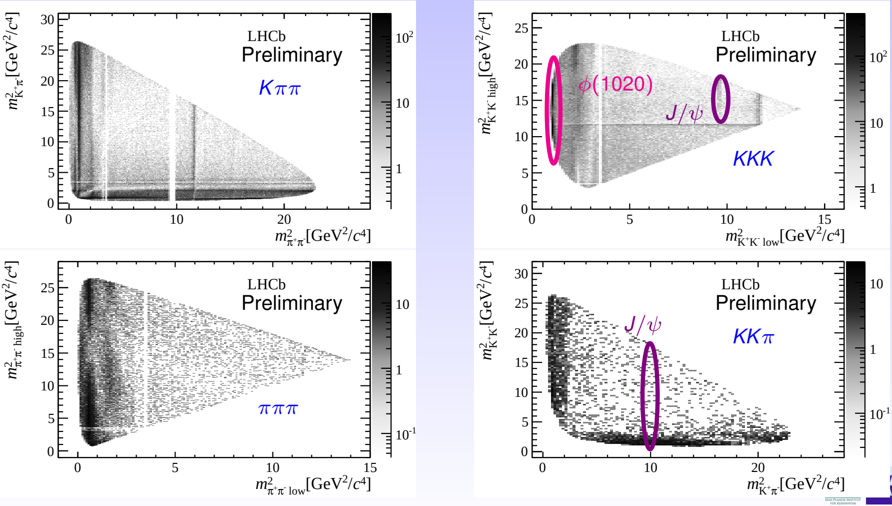

CP asymmetries in the phase space [LHCb-PAPER-2014-044 Preliminary]

NEW

- Asymmetries in bins of the Dalitz plot: background subtracted and efficiency corrected
- Binning chosen adaptively: $\sim$ equal $(N^+ + N^-)$ in each bin

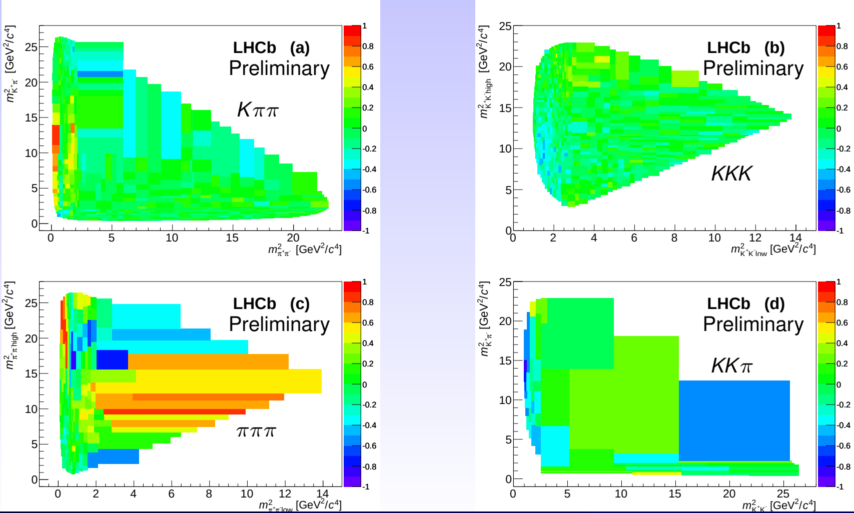

CP asymmetries in the phase space [LHCb-PAPER-2014-044 Preliminary]

NEW

Large positive asymmetries at low $m^2_{\pi\pi}$

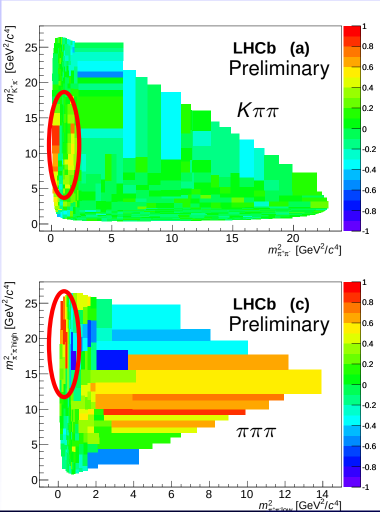

Large negative asymmetries at low m^2_{KK}

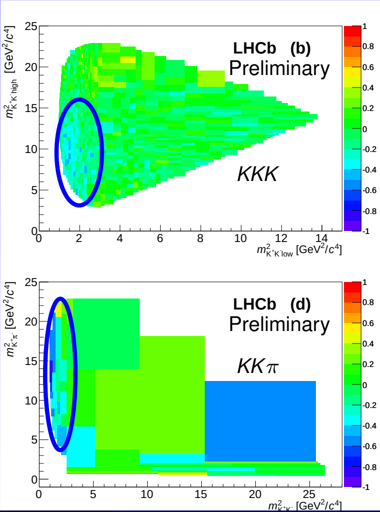

CP asymmetries in the phase space [LHCb-PAPER-2014-044 Preliminary]

NEW

Two sources of CP violation:

1) $\pi^{+}\pi^{-} \leftrightarrow K^{+}K^{-}$ **rescattering** appearing with different sign asymmetries

2) **Final-state strong interference** (FSI) between S-wave and P-wave

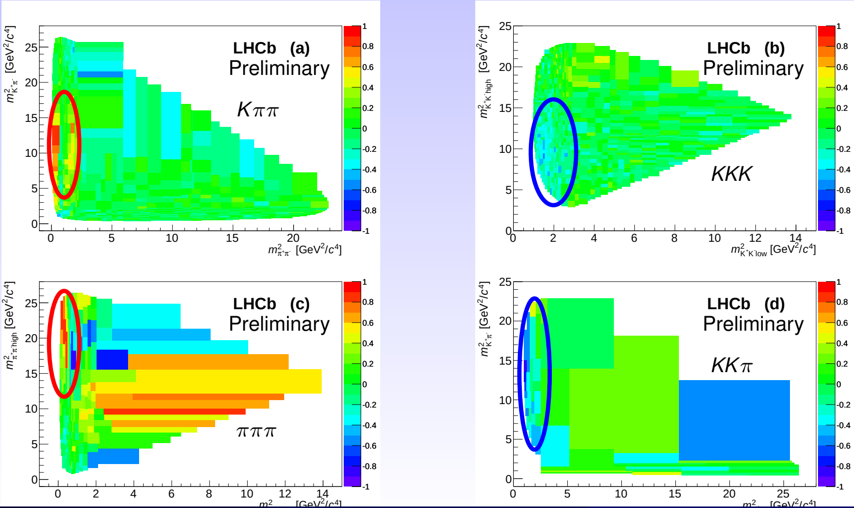

Two-body projections [LHCb-PAPER-2014-044 Preliminary]

NEW

- Projections on the m_{hh} splitted according to the sign of the cosine of the angle between the momenta of the unpaired hadron and the resonant daughter with the same-sign charge

$B^{\pm} \to \pi^{+}\pi^{-}\pi^{\pm}$

$B^{\pm} \to K^{+}K^{-}K^{\pm}$

$\cos\theta < 0$

$\cos\theta > 0$

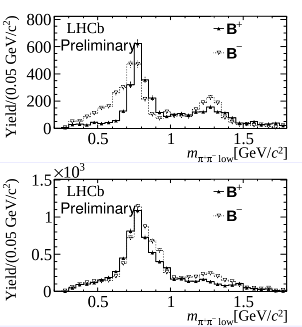

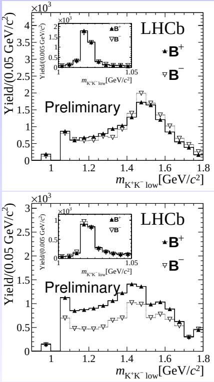

- First source of CP violation evident in the region $(1.0 - 1.5)GeV/c^2$ where large asymmetries are observed (also in the other channels)
- **CPT**: the sum of partial width of a family of final states related by strong rescattering should be the same for particles and antiparticles $\Rightarrow$ positive and negative asymmetries

Two-body projections [LHCb-PAPER-2014-044 Preliminary]

NEW

- Projections on the m_{hh} splitted according to the sign of the cosine of the angle between the momenta of the unpaired hadron and the resonant daughter with the same-sign charge

$B^{\pm} \to \pi^+ \pi^- \pi^{\pm}$

$B^{\pm} \to K^+ K^- K^{\pm}$

$\cos\theta < 0$

$\cos\theta > 0$

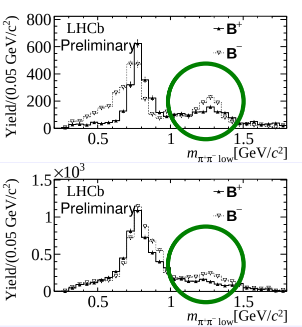

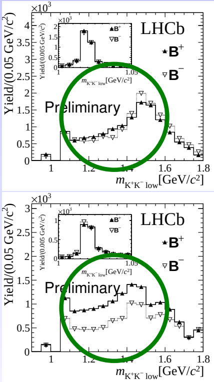

- First source of CP violation evident in the region $(1.0 - 1.5) GeV/c^2$ where large asymmetries are observed (also in the other channels)
- **CPT**: the sum of partial width of a family of final states related by strong rescattering should be the same for particles and antiparticles $\Rightarrow$ positive and negative asymmetries

CPV induced by rescattering [LHCb-PAPER-2014-044 Preliminary]

NEW

Invariant masses with $\pi\pi$ and KK in the "**rescattering region**": $(1.0-1.5)GeV/c^2$ [PRD 22 (1980) 2595] [NPB 158 (1979) 23 520]

$\mathcal{A}_{CP}(K\pi\pi) = +0.121 \pm 0.012 \pm 0.017 \pm 0.007$

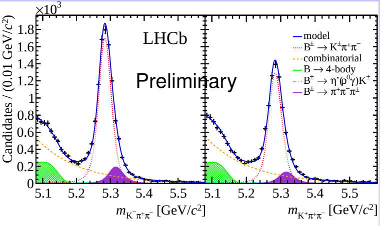

$\mathcal{A}_{CP}(KKK) = -0.211 \pm 0.011 \pm 0.004 \pm 0.007$

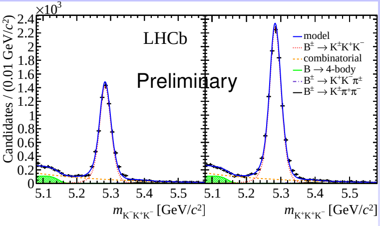

$\mathcal{A}_{CP}(\pi\pi\pi) = +0.172 \pm 0.021 \pm 0.015 \pm 0.007$

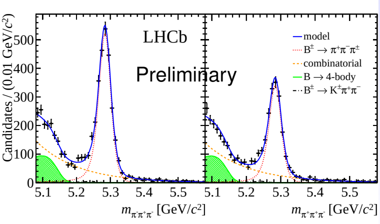

$\mathcal{A}_{CP}(\pi KK) = -0.328 \pm 0.028 \pm 0.029 \pm 0.007$

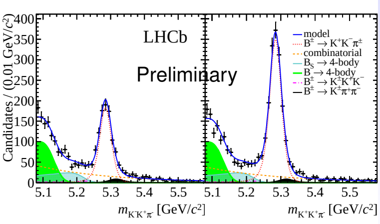

All the asymmetries have more than 5σ of significance

Charge asymmetries [LHCb-PAPER-2014-044 Preliminary]

NEW

- Charge asymmetries splitted according to $\cos\theta$

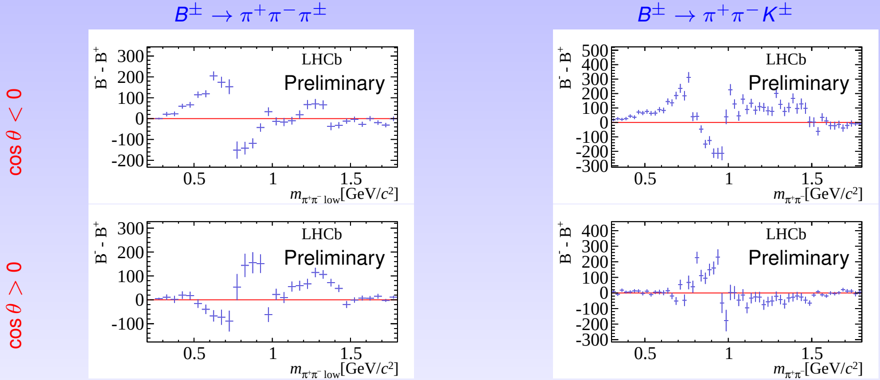

- The interference term $\propto \cos\theta$ [-1,1]: interference changes sign
- The charge asymmetry changes sign near the resonances: dominance of the long-distance interference
- For $\pi\pi\pi$ the change of sign occurs for both $\cos\theta > 0$ and $\cos\theta < 0$: asymmetry related to the real part of the long-distance interference
- For $\pi\pi K$ only the $f_0(980)$ presents both zeros

Charge asymmetries [LHCb-PAPER-2014-044 Preliminary]

NEW

- Charge asymmetries splitted according to $\cos\theta$

$B^{\pm} \to \pi^+ \pi^- \pi^{\pm}$

$B^{\pm} \to \pi^+ \pi^- K^{\pm}$

$\cos\theta < 0$

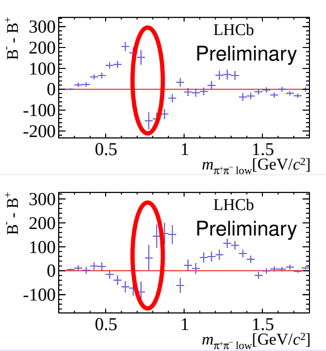

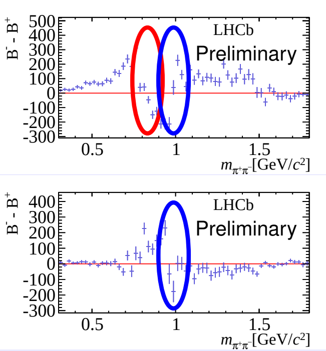

$\cos\theta > 0$

- The interference term $\propto \cos\theta$ [-1,1]: interference changes sign
- The charge asymmetry changes sign near the resonances: dominance of the long-distance interference
- For $\pi\pi\pi$ the change of sign occurs for both $\cos\theta > 0$ and $\cos\theta < 0$: asymmetry related to the real part of the long-distance interference
- For $\pi\pi K$ only the $f_0(980)$ presents both zeros

CPV induced by interference [LHCb-PAPER-2014-044 Preliminary]

NEW

$\rho(770)$ **region** divided into four sectors depending on $m_{\pi\pi}$ and the cosine of the angle between the momenta of the unpaired hadron and the resonant daughter with the same-sign charge

$0.47 < m_{\pi\pi\,low}\,GeV/c^2 < 0.77$ | $0.77 < m_{\pi\pi\,low}\,GeV/c^2 < 0.92$

$\cos\theta > 0$

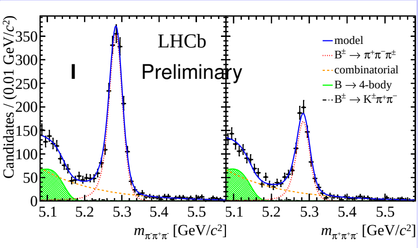

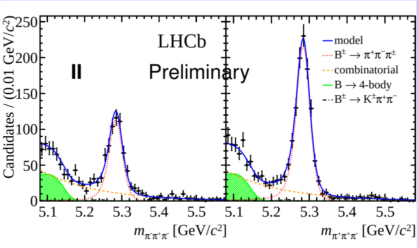

$\cos\theta < 0$

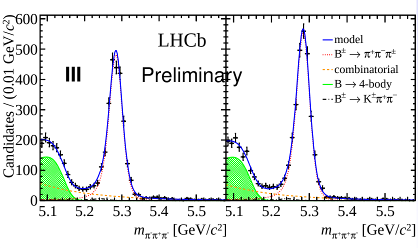

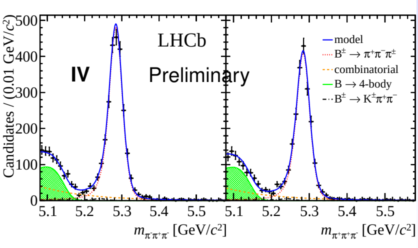

CPV induced by interference [LHCb-PAPER-2014-044 Preliminary]

NEW

Charge asymmetries measured in the four sectors for various vector resonances:

Preliminary

Decay mode	Resonance	Sector	N_s	$A_{CP} \pm \sigma_{(stat)} \pm \sigma_{(syst)} \pm \sigma_{(J/\psi K^{\pm})}$
$B^{\pm} \to K^{\pm}\pi^{+}\pi^{-}$	ρ	I	2909 ± 80	$-0.052 \pm 0.032 \pm 0.047 \pm 0.007$
		II	6136 ± 100	$+0.140 \pm 0.018 \pm 0.034 \pm 0.007$
		III	2856 ± 86	$+0.598 \pm 0.036 \pm 0.079 \pm 0.007$
		IV	2107 ± 55	$-0.208 \pm 0.043 \pm 0.042 \pm 0.007$
$B^{\pm} \to K^{\pm}\pi^{+}\pi^{-}$	K^{*}	I	11095 ± 115	$+0.002 \pm 0.013 \pm 0.011 \pm 0.007$
		II	7159 ± 89	$+0.007 \pm 0.016 \pm 0.005 \pm 0.007$
		III	2427 ± 65	$-0.009 \pm 0.031 \pm 0.054 \pm 0.007$
		IV	9861 ± 124	$-0.020 \pm 0.015 \pm 0.010 \pm 0.007$
$B^{\pm} \to \pi^{\pm}\pi^{+}\pi^{-}$	ρ	I	2629 ± 59	$+0.302 \pm 0.026 \pm 0.015 \pm 0.007$
		II	1653 ± 46	$-0.244 \pm 0.034 \pm 0.019 \pm 0.007$
		III	5204 ± 79	$-0.076 \pm 0.019 \pm 0.007 \pm 0.007$
		IV	4476 ± 72	$+0.055 \pm 0.020 \pm 0.013 \pm 0.007$
$B^{\pm} \to K^{\pm}K^{+}K^{-}$	ϕ	I	3082 ± 56	$-0.018 \pm 0.024 \pm 0.008 \pm 0.007$
		II	4119 ± 64	$-0.008 \pm 0.021 \pm 0.004 \pm 0.007$
		III	1546 ± 39	$+0.066 \pm 0.034 \pm 0.010 \pm 0.007$
		IV	2719 ± 53	$+0.015 \pm 0.026 \pm 0.002 \pm 0.007$

Significant CP asymmetry in the decays involving a $\rho(770)$

$B^{\pm} \rightarrow p\bar{p}h^{\pm}$ decays

Direct CPV in $B^{\pm} \to p\bar{p}h^{\pm}$

LHCb-PAPER-2014-034 in preparation

- **Motivation**:
  - Large CPV observed in $B^{\pm} \to h^{+}h^{-}h^{\pm}$decays
  - Hadron rescattering $hh \to pp$ not expected to play a large role compared to $\pi\pi \to KK$: expect smaller CPV
- **Analysis** uses 3 fb^{-1} of data recorded by LHCb in 2011 and 2012:
  - Selection strategy similar to $B^{\pm} \to h^{+}h^{-}h^{\pm}$analysis and improved w.r.t. the previous publication [PRD 88 (2013) 052015]
- **Measurements**:
  - CP violation in phase space
  - Forward-backward asymmetry
  - BR measurement of the $B^{+} \to \bar{\Lambda}(1520)(\to \bar{p}K)p$ decay

Direct CPV in $B^{\pm} \to p\bar{p}h^{\pm}$ [LHCb-PAPER-2014-034 (PRELIMINARY)]

NEW

- Yields extracted with an unbinned maximum likelihood fit

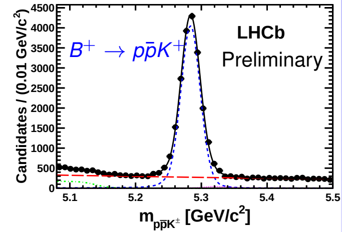

$N = 18721 \pm 142$

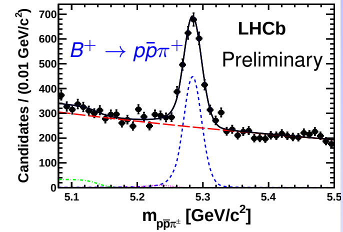

$N = 1988 \pm 74$

- Background subtracted Dalitz distributions using signal sWeight

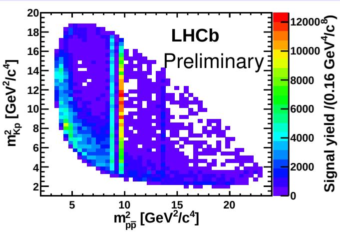

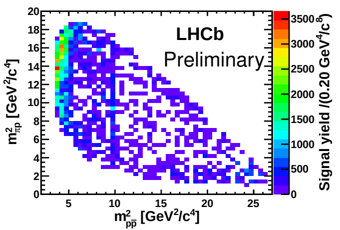

Dalitz plots [LHCb-PAPER-2014-034 (PRELIMINARY)]

NEW

- Background subtracted Dalitz distributions using sPlot technique

$B^+ \to p\bar{p}K^+$

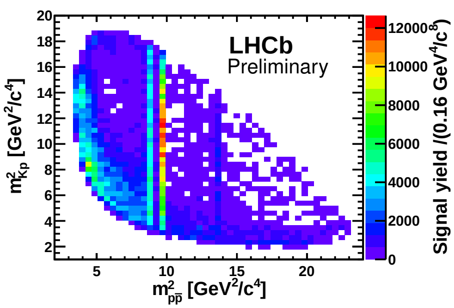

$B^+ \to p\bar{p}\pi^+$

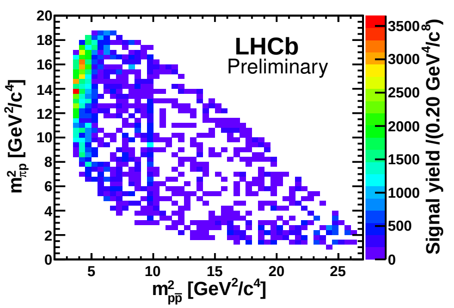

Dalitz plots [LHCb-PAPER-2014-034 (PRELIMINARY)]

NEW

- Background subtracted Dalitz distributions using sPlot technique

$B^{+} \to p\bar{p}K^{+}$ $B^{+} \to p\bar{p}\pi^{+}$

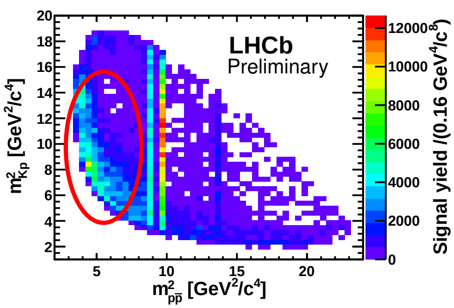

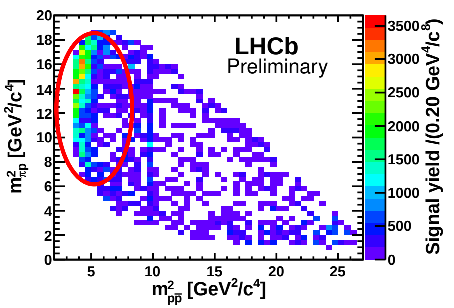

- Enhancement at low $m^2_{p\bar{p}}$ invariant mass differently distributed in the two modes

Dalitz plots [LHCb-PAPER-2014-034 (PRELIMINARY)]

NEW

- Background subtracted Dalitz distributions using sPlot technique

$B^+ \to p\bar{p}K^+$

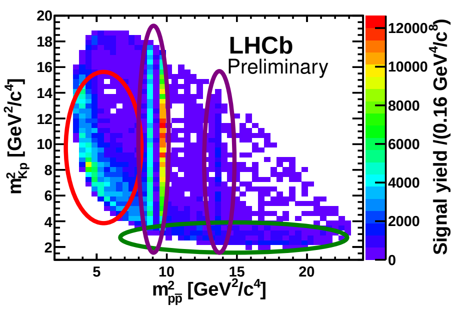

$B^+ \to p\bar{p}\pi^+$

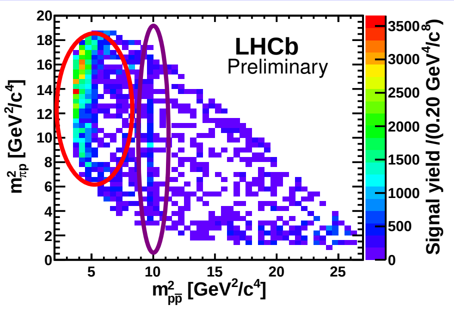

- Enhancement at low $m^2_{p\bar{p}}$ invariant mass differently distributed in the two modes
- Charmonium bands clearly visible:
  - $J\psi$, $\psi(2S)$ and η_c
- $\Lambda(1520) \to pK$

Dynamics of $B^\pm \to p\bar{p}h^\pm$ decays [LHCb-PAPER-2014-034 (PRELIMINARY)]

- Dynamics in the charmless region: $m_{p\bar{p}} < 2.85 GeV/c^2$
- Acceptance-corrected distribution of the cosine of the helicity angle θ_p of the $p\bar{p}$ system

$B^+ \to p\bar{p}K^+$

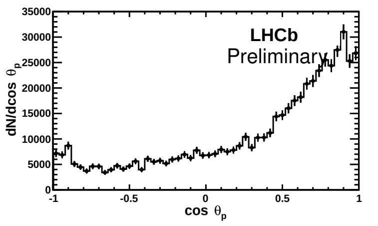

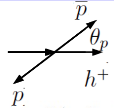

$B^+ \to p\bar{p}\pi^+$

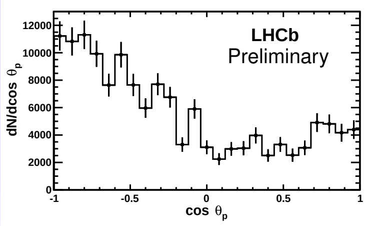

- Opposite behaviour of the two modes:
  can be generated by non-resonant scattering [J.Phys. G34 (2007) 283]

Dynamics of $B^{\pm} \to p\bar{p}h^{\pm}$ decays [LHCb-PAPER-2014-034 (PRELIMINARY)]

- Measurement of the forward-backward asymmetry

$$\mathcal{A}_{FB} = \frac{N(\cos\theta_p > 0) - N(\cos\theta_p < 0)}{N(\cos\theta_p > 0) + N(\cos\theta_p < 0)}$$

- Variation of the A_{FB} in function of $m_{p\bar{p}}$

$B^+ \to p\bar{p}K^+$

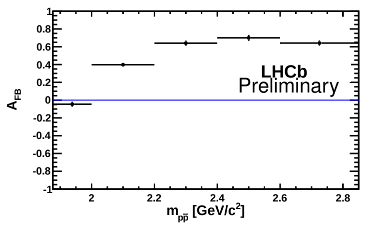

$B^+ \to p\bar{p}\pi^+$

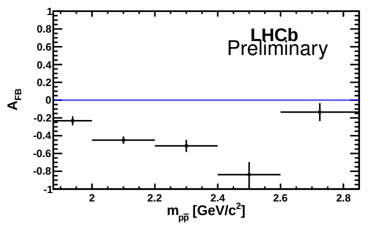

- Opposite behaviour for the two decay modes

Preliminary

$$\mathcal{A}_{FB}(p\bar{p}K^+, m_{p\bar{p}} < 2.85 GeV/c^2) = 0.495 \pm 0.012(stat) \pm 0.007(syst)$$
$$\mathcal{A}_{FB}(p\bar{p}\pi^+, m_{p\bar{p}} < 2.85 GeV/c^2) = -0.409 \pm 0.033(stat) \pm 0.006(syst)$$

- Improvement with respect to Belle [PLB 659 (2008) 80]

CP asymmetries [LHCb-PAPER-2014-034 (PRELIMINARY)]

- Variation of A_{CP} as a function of the Dalitz-plot variables only for $B^{\pm} \to p\bar{p}K^{\pm}$
- Adaptive binning analysis

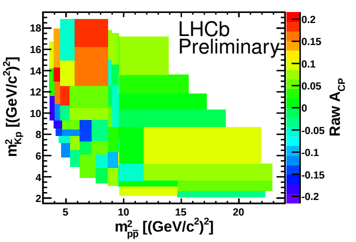

CP asymmetries [LHCb-PAPER-2014-034 (PRELIMINARY)]

- Variation of A_{CP} as a function of the Dalitz-plot variables only for $B^{\pm} \to p\bar{p}K^{\pm}$
- Adaptive binning analysis

$m^2_{Kp} > 10\ GeV^2/c^4$

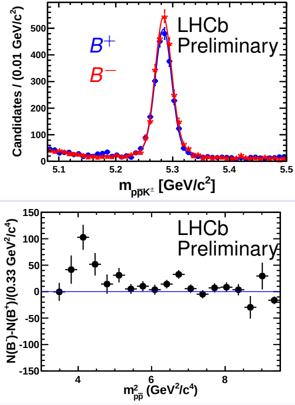

Clear sign-flip pattern at low $m^2_{p\bar{p}}$

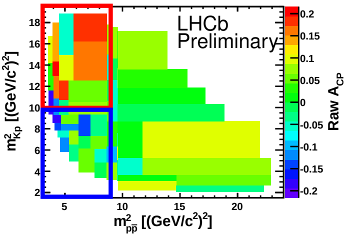

$m^2_{Kp} < 10\ GeV^2/c^4$

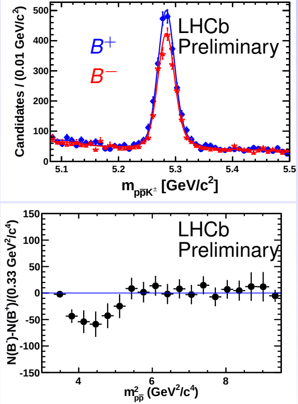

CP asymmetries [LHCb-PAPER-2014-034 (PRELIMINARY)]

NEW

- The raw CP is corrected for production and detection asymmetries

$$B^\pm \to p\bar{p}K^\pm \qquad \mathcal{A}_{CP} = \mathcal{A}_{raw} - \mathcal{A}_P(B^\pm) - \mathcal{A}_D(K^\pm)$$
$$B^\pm \to p\bar{p}\pi^\pm \qquad \mathcal{A}_{CP} = \mathcal{A}_{raw} - \mathcal{A}_P(B^\pm) - \mathcal{A}_D(\pi^\pm)$$

  - $\mathcal{A}_P(B^\pm) + \mathcal{A}_D(K^\pm)$ obtained using $B^\pm \to J/\psi(p\bar{p})K^\pm$
  - $\mathcal{A}_D(\pi^\pm)$ taken from studies of prompt D^+ decays [LHCb - arXiv:1405.2797]

First evidence of CPV in baryonic B decays

Preliminary

Mode/region	A_{CP}	
$\eta_c(\to p\bar{p})K^\pm$	0.040±0.034 (stat)±0.004 (syst)	
$\psi(2S)(\to p\bar{p})K^\pm$	0.092±0.058 (stat)±0.004 (syst)	
$p\bar{p}K^\pm,\ m_{p\bar{p}} < 2.85\ \mathrm{GeV}/c^2$	0.021±0.020 (stat)±0.004 (syst)	
$p\bar{p}K^\pm,\ m_{p\bar{p}} < 2.85\ \mathrm{GeV}/c^2,\ m^2_{Kp} < 10\ \mathrm{GeV}^2/c^4$	-0.036±0.023 (stat)±0.004 (syst)	
$p\bar{p}K^\pm,\ m_{p\bar{p}} < 2.85\ \mathrm{GeV}/c^2,\ m^2_{Kp} > 10\ \mathrm{GeV}^2/c^4$	0.096±0.024 (stat)±0.004 (syst)	4σ
$p\bar{p}K^\pm,\ m^2_{p\bar{p}} < 6\ \mathrm{GeV}^2/c^4,\ m^2_{Kp} < 10\ \mathrm{GeV}^2/c^4$	-0.066±0.026 (stat)±0.004 (syst)	
$p\bar{p}K^\pm,\ m^2_{p\bar{p}} < 6\ \mathrm{GeV}^2/c^4,\ m^2_{Kp} > 10\ \mathrm{GeV}^2/c^4$	0.087±0.026 (stat)±0.004 (syst)	3.5σ
$p\bar{p}\pi^\pm,\ m_{p\bar{p}} < 2.85\ \mathrm{GeV}/c^2$	-0.041±0.039 (stat)±0.005 (syst)	

- Systematics uncertainties dominated by the uncertainty on the $\mathcal{A}_{CP}(J/\psi K)$ measurement

Branching fraction measurements [LHCb-PAPER-2014-034 (PRELIMINARY)]

NEW

- Branching fraction of $B^+ \to \bar{\Lambda}(1520)(K^+\bar{p})p$ relative to $B^+ \to J/\psi(p\bar{p})K^+$

$$\frac{\mathcal{B}(B^+ \to \bar{\Lambda}(1520)(K^+\bar{p})p)}{\mathcal{B}(B^+ \to J/\psi(p\bar{p})K^+)} = \frac{N_{\Lambda\to Kp}}{N_{J/\psi\to p\bar{p}}} \times \frac{\epsilon^{gen}_{J/\psi\to p\bar{p}}}{\epsilon^{gen}_{\Lambda\to Kp}} \times \frac{\epsilon^{sel}_{J/\psi\to p\bar{p}}}{\epsilon^{sel}_{\Lambda\to Kp}}$$

- Similar equation for the ratio $B^+ \to p\bar{p}\pi^+$ to $B^+ \to J/\psi(p\bar{p})\pi^+$
- Resonant modes extracted with a 2D fit to $p\bar{p}h^+$ and $p\bar{p}/K^+\bar{p}$

Preliminary

$$\frac{\mathcal{B}(B^+\to\bar{\Lambda}(1520)(K^+\bar{p})p)}{\mathcal{B}(B^+\to J/\psi(p\bar{p})K^+)} = 0.033 \pm 0.005(stat) \pm 0.007(syst)$$

$$\frac{\mathcal{B}(B^+\to p\bar{p}\pi^+), m_{p\bar{p}}<2.85 GeV/c^2}{\mathcal{B}(B^+\to J/\psi(p\bar{p})\pi^+)} = 12.0 \pm 1.2(stat) \pm 0.3(syst)$$

- Using
  - $\mathcal{B}(B^+ \to J/\psi K^+) = (1.016 \pm 0.033) \times 10^{-3}$ [PDG]
  - $\mathcal{B}(J/\psi \to p\bar{p}) = (2.17 \pm 0.07) \times 10^{-3}$ [PDG]
  - $\mathcal{B}(\Lambda(1520) \to K^+\bar{p}) = 0.234 \pm 0.016$ [Eur.Phys.J. A47(2011)133]

Preliminary

$$\mathcal{B}(B^+ \to \bar{\Lambda}(1520)(K^+\bar{p})p) = (3.15 \pm 0.48(stat) \pm 0.07(syst) \pm 0.26(BF)) \times 10^{-7}$$
$$\mathcal{B}(B^+ \to p\bar{p}\pi^+, m_{p\bar{p}} < 2.85 GeV/c^2) = (1.07 \pm 0.11(stat) \pm 0.03(syst) \pm 0.11(BF)) \times 10^{-6}$$

Conclusions

- Measurement of CPV in the $B^{\pm} \to h^{+}h^{-}h^{\pm}$ decays (3 fb^{-1})
  - The inclusive measurement is consistent and supersedes the previous LHCb results
  - The CP asymmetries in the phase space are not distributed uniformly
  - The long-distance $\pi\pi \to KK$ rescattering is important, but the role of the unpaired hadron has to be better understood
  - The CP asymmetry related in the $\rho(770)$ region may be related to the real part of the long-distance interactions between the S-wave and P-wave contributions
- Measurement of CPV in the $B^{\pm} \to p\bar{p}h^{\pm}$ decays (3 fb^{-1})
  - Indication of a sign-flip pattern of the CP asymmetry at low $m_{p\bar{p}}$
  - The strong phase difference is probably generated by the interference of long-distance $p\bar{p}$ waves
  - First evidence of CPV in baryonic B decays in $B^{\pm} \to p\bar{p}K^{\pm}$
  - Improved measurement of the $B^{+} \to \bar{\Lambda}(1520)(\to \bar{p}K)p$ BF
- A comprehensive study of these phenomenons has to be conducted with an amplitude analysis, currently underway and will receive soon updates!!

Conclusions

- Measurement of CPV in the $B^\pm \to h^+ h^- h^\pm$ decays (3 fb^{-1})
  - The inclusive measurement is consistent and supersedes the previous LHCb results
  - The CP asymmetries in the phase space are not distributed uniformly
  - The long-distance $\pi\pi \to KK$ rescattering is important, but the role of the unpaired hadron has to be better understood
  - The CP asymmetry related in the $\rho(770)$ region may be related to the real part of the long-distance interactions between the S-wave and P-wave contributions
- Measurement of CPV in the $B^\pm \to p\bar{p}h^\pm$ decays (3 fb^{-1})
  - Indication of a sign-flip pattern of the CP asymmetry at low $m_{p\bar{p}}$
  - The strong phase difference is probably generated by the interference of long-distance $p\bar{p}$ waves
  - First evidence of CPV in baryonic B decays in $B^\pm \to p\bar{p}K^\pm$
  - Improved measurement of the $B^+ \to \bar{\Lambda}(1520)(\to \bar{p}K)p$ BF
- A comprehensive study of these phenomenons has to be conducted with an amplitude analysis, currently underway and will receive soon updates!!

Thanks for your attention!

Backup slides

LHCb detector

Single arm spectrometer for precision measurement of CP violation and rare B decays

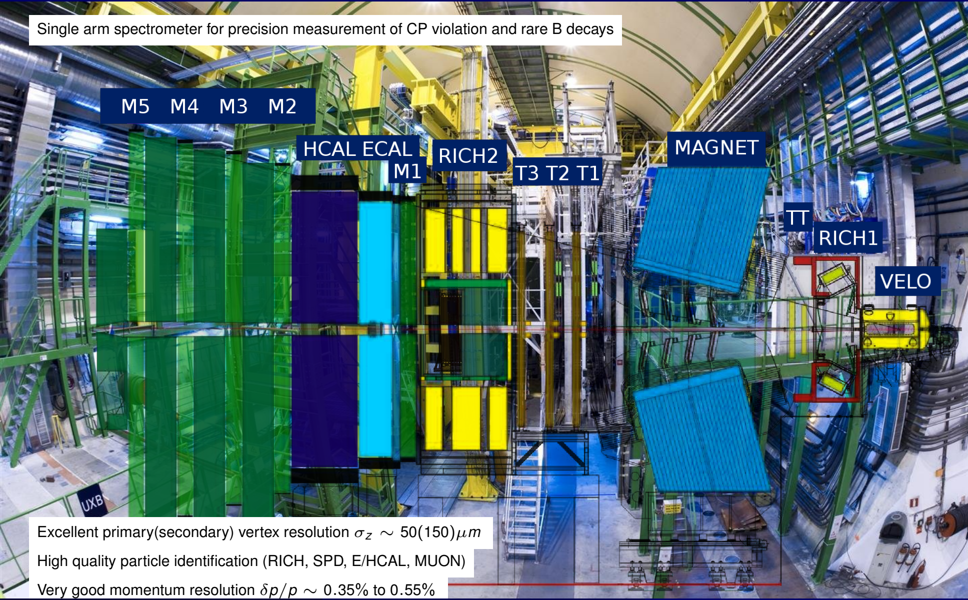

Excellent primary(secondary) vertex resolution $\sigma_z \sim 50(150)\mu m$

High quality particle identification (RICH, SPD, E/HCAL, MUON)

Very good momentum resolution $\delta p/p \sim 0.35\%$ to 0.55%

Two-body projections [LHCb-PAPER-2014-044 Preliminary]

NEW

- Projections on the $m_{\pi\pi}$ splitted according to the sign of the cosine of the angle between the momenta of the unpaired hadron and the resonant daughter with the same-sign charge

$B^{\pm} \to \pi^+\pi^-\pi^{\pm}$ | $B^{\pm} \to \pi^+\pi^-K^{\pm}$

$\cos\theta < 0$

$\cos\theta > 0$

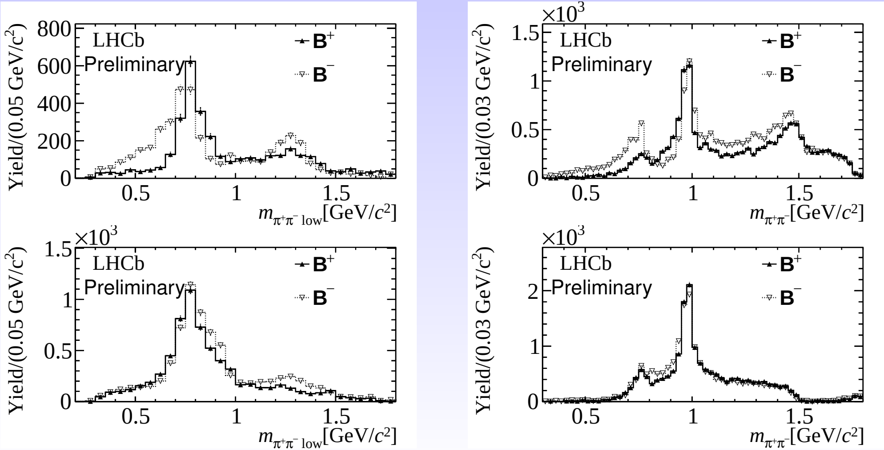

Two-body projections [LHCb-PAPER-2014-044 Preliminary]

NEW

- Projections on the $m_{\pi\pi}$ splitted according to the sign of the cosine of the angle between the momenta of the unpaired hadron and the resonant daughter with the same-sign charge

$B^{\pm} \to \pi^{+}\pi^{-}\pi^{\pm}$ $\quad$ $B^{\pm} \to \pi^{+}\pi^{-}K^{\pm}$

$\cos\theta < 0$

$\cos\theta > 0$

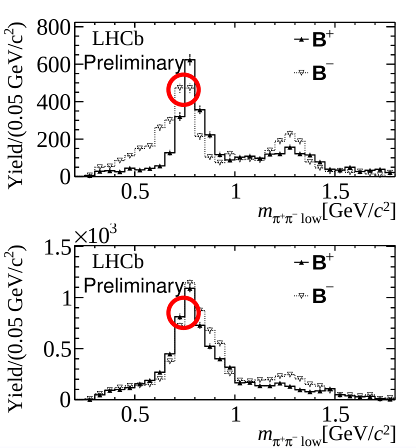

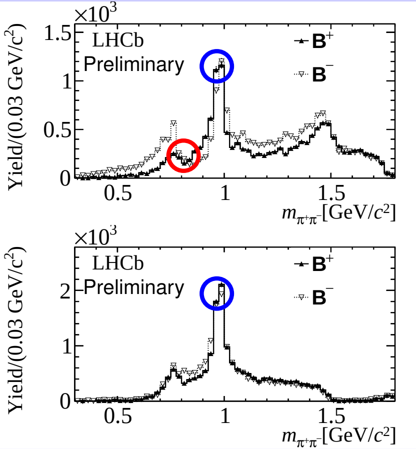

Two-body projections [LHCb-PAPER-2014-044 Preliminary]

NEW

- Projections on the m_{KK} splitted according to the sign of the cosine of the angle between the momenta of the unpaired hadron and the resonant daughter with the same-sign charge

$B^{\pm} \to K^+ K^- K^{\pm}$

$\cos\theta < 0$

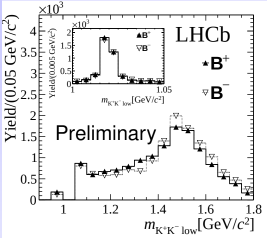

$\cos\theta > 0$

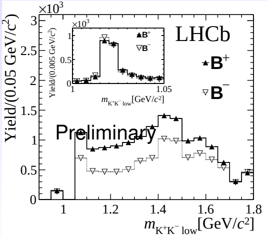

$B^{\pm} \to K^+ K^- \pi^{\pm}$

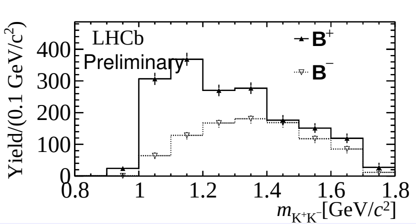

A. Gomez

Theory Overview I

$B^{\pm} \to K^{\pm}\pi^{+}\pi^{-}$ BR ∝ 10^{-5}

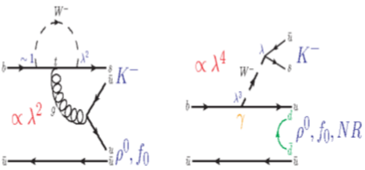

$B^{\pm} \to K^{\pm}K^{+}K^{-}$ BR ∝ 10^{-5}

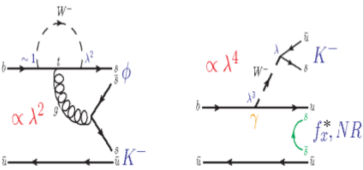

- Access to t → s (P) and the CKM phase b → u (T) transitions.
  - γ at tree level.
- CP violation (CPV) expected from interference between tree (∝ λ^4) and penguin (∝ λ^2) diagrams in both channels. Type I
- For Kππ:
  - CP violation expected also from ρ^0, f_0 and K* interferences in the phase space. Type II
- For KKK:
  - φ resonance only from penguin contribution.
  - CPV expected only from interference between φ and f_x (or no-resonant). Type II
- Note that Type I and Type II are two different sources of CPV.

* fx holds for any resonance with the K^+K^- final state.

3

A. Gomez

Theory Overview II

$B^{\pm} \to \pi^{\pm}\pi^{+}\pi^{-}$ BR $\propto 10^{-5}$

$B^{\pm} \to \pi^{\pm}K^{+}K^{-}$ BR $\propto 10^{-6}$

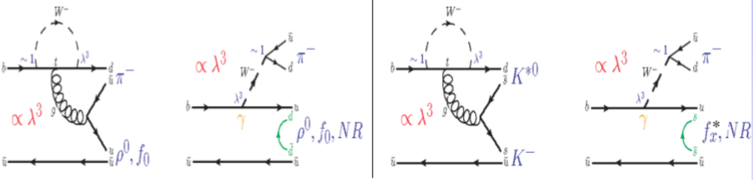

- Access to $t \to d$ (P) and the CKM phase $b \to u$ (T) transitions.
  - γ at tree level.
- CPV expected from interference between tree ($\propto \lambda^3$) and penguin ($\propto \lambda^3$) diagrams in both channels. Type I
- For πππ:
  - CP violation expected also from ρ^0 and f_0 interferences in the phase space. Type II
- For πKK:
  - φ resonance not expected for this mode (for current LHCb statistics).
  - CPV expected only from interference between K* and f_x (or no-resonant). Type II
- Note that Type I and Type II are two different sources of CPV.

* fx holds for any resonance with the K^+K^- final state.

4

One resonance and non-resonance amplitude

- $B \to \pi\pi\pi$ at low $m_{\pi\pi} \implies \rho(770)$ and non resonant amplitude
- Breit-Wigner excitation curve for a resonance R

$$F_R^{\mathrm{BW}}(s) = \frac{1}{m_R^2 - s - i m_R \Gamma_R(s)} \ ,$$

- Real and imaginary part

$$\mathbf{Re}F_R^{\mathrm{BW}}(s) = \frac{m_R^2 - s}{(m_R^2 - s)^2 + m_R^2 \Gamma_R(s)^2} \ ,$$

$$\mathbf{Im}F_R^{\mathrm{BW}}(s) = \frac{m_R \Gamma_R(s)}{(m_R^2 - s)^2 + m_R^2 \Gamma_R(s)^2} \ ,$$

- The square amplitude is

$$|F_R^{\mathrm{BW}}(s)|^2 = \frac{1}{(m_R^2 - s)^2 + m_R^2 \Gamma_R(s)^2} \ ,$$

- The amplitudes for B^+ and B^- can be written as

$$\begin{aligned} \mathcal{M}_+ &= a_+^\rho e^{i\delta_+^\rho} F_\rho^{\mathrm{BW}} \cos\theta + a_+^{nr} e^{i\delta_+^{nr}} F^{\mathrm{NR}}, \\ \mathcal{M}_- &= a_-^\rho e^{i\delta_-^\rho} F_\rho^{\mathrm{BW}} \cos\theta + a_-^{nr} e^{i\delta_-^{nr}} F^{\mathrm{NR}}, \end{aligned}$$

  - F^{NR} is a real and scalar non-resonant amplitude
  - $\delta_\pm$ contains both the fixed weak and the strong phases
  - F^{BW} introduce additional mass dependent strong phases

One resonance and non-resonance amplitude

- The subtraction of the square modulus of the amplitude is

$$\begin{aligned}\Delta|\mathcal{M}^2| &= |\mathcal{M}_+|^2 - |\mathcal{M}_-|^2 \\ &= [(a_+^\rho)^2 - (a_-^\rho)^2]|F_\rho^{\rm BW}|^2 \cos^2\theta + [(a_+^{nr})^2 - (a_-^{nr})^2]|F^{\rm NR}|^2 + 2\cos\theta|F_\rho^{\rm BW}|^2|F^{\rm NR}|^2 \times \\ &\quad \{(m_\rho^2 - s)\,[a_+^\rho a_+^{nr}(\cos(\delta_+^\rho - \delta_+^{nr}) - a_-^\rho a_-^{nr}\cos(\delta_-^\rho - \delta_-^{nr})] \\ &\quad -m_\rho\Gamma_\rho\,[a_+^\rho a_+^{nr}(\sin(\delta_+^\rho - \delta_+^{nr}) - a_-^\rho a_-^{nr}\sin(\delta_-^\rho - \delta_-^{nr})]\}. \qquad (54)\end{aligned}$$

  - The first two terms are associated to the direct CP violation
  - The others are related to the Dalitz interference between neighbors resonances (DCPV) with two contributions
    - Real part
    - Imaginary part

- The first term is equivalent to the direct CPV induced by the short distance interference between the tree and penguin amplitudes in a same intermediary state
- The real term is related with the real part of the BW
- The imaginary term is related to the imaginary part of the BW

One resonance and non-resonance amplitude

- The first term is equivalent to the direct CPV induced by the short distance interference between the tree and penguin amplitudes in a same intermediary state

$$[(a_+^\rho)^2 - (a_-^\rho)^2]|F_\rho^{\mathrm{BW}}|^2 \cos^2\theta$$

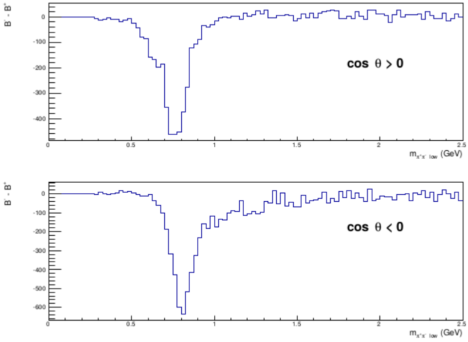

Figure 21: A simulation of CP violation for the $B^\pm \to \pi^\pm\pi^+\pi^+$ decay, with only contribution of directly CP violation. The figure on top corresponds to the events with $\cos\theta > 0$; the bottom one $\cos\theta < 0$.

One resonance and non-resonance amplitude

- The real term is related with the real part of the BW. The projection of the difference between positive and negative square amplitude presents a clear signature in the mass spectrum, a zero and a change of sign of the CP violation at the central value of the mass of the resonance.

$$2\cos\theta|F_{\rho}^{\rm BW}|^2|F^{\rm NR}|^2\,(m_{\rho}^2 - s)$$

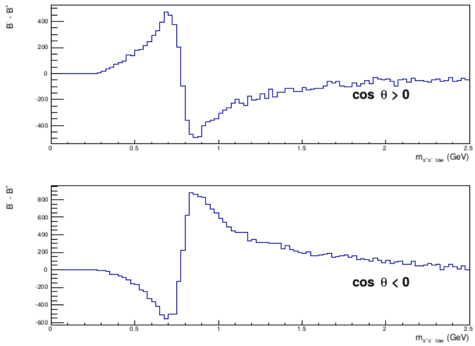

Figure 22: A simulation of *CP* violation for the $B^{\pm} \to \pi^{\pm}\pi^{+}\pi^{+}$ decay, with only contribution of the real part of Dalitz interference CP violation. The figure on top corresponds to the events with $\cos\theta > 0$; the bottom one $\cos\theta < 0$.

One resonance and non-resonance amplitude

- The imaginary term is related to the imaginary part of the BW. The shape is similar to the directly term but the proportionality with *cosθ* changes the signal of the CP violation when *cosθ* pass through zero at the middle of the Dalitz plot

$$2\cos\theta|F_\rho^{\mathrm{BW}}|^2|F^{\mathrm{NR}}|^2\, m_\rho\Gamma_\rho$$

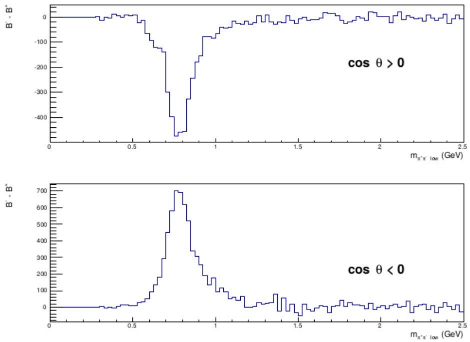

Figure 23: A simulation of *CP* violation for the $B^\pm \to \pi^\pm\pi^+\pi^+$ decay, with only contribution of the imaginary part of Dalitz interference CP violation. The figure on top corresponds to the events with $\cos\theta > 0$; the bottom one $\cos\theta < 0$.

Scalar and vector resonances

- The non-resonant amplitude is replaced by a scalar resonant amplitude, for instance the $\rho(770)$ and $f_0(980)$
- The amplitudes for B^+ and B^- can be written as

$$\begin{aligned}\mathcal{M}_+ &= a_+^\rho e^{i\delta_+^\rho} F_\rho^{\rm BW}\cos\theta + a_+^{nr} e^{i\delta_+^{nr}} F^{\rm NR},\\ \mathcal{M}_- &= a_-^\rho e^{i\delta_-^\rho} F_\rho^{\rm BW}\cos\theta + a_-^{nr} e^{i\delta_-^{nr}} F^{\rm NR},\end{aligned}$$

- The subtraction of the square modulus of the amplitude is

$$\begin{aligned}|\Delta\mathcal{M}|^2 &= |\mathcal{M}_+|^2 - |\mathcal{M}_-|^2\\ &= [(a_+^\rho)^2 - (a_-^\rho)^2]|F_\rho^{\rm BW}|^2\cos^2\theta + [(a_+^f)^2 - (a_-^f)^2]|F_f^{\rm BW}|^2 + 2\cos\theta|F_\rho^{\rm BW}|^2|F_f^{\rm BW}|^2\times\\ &\quad \{[(m_\rho^2 - s)(m_f^2 - s) - m_\rho\Gamma_\rho m_f\Gamma_f][a_+^\rho a_+^f\cos(\delta_+^\rho - \delta_+^f) - a_-^\rho a_-^f\cos(\delta_-^\rho - \delta_-^f)]\\ &\quad -[m_\rho\Gamma_\rho(m_f^2 - s) - m_f\Gamma_f(m_\rho^2 - s))[a_+^\rho a_+^f\sin(\delta_+^\rho - \delta_+^f) - a_-^\rho a_-^f\sin(\delta_-^\rho - \delta_-^f)]\}\end{aligned} \tag{57}$$

- There are four terms again, where the direct CP violation is completely equivalent to the previous study
- The main difference derive from the additional terms that appear in both interference terms
- Note that the real contribution has two zeros: one related to the ρ and the other to the $f_0(980)$
- They should not have their zeros at the nominal mass. However the additional term is not large mainly because it involves the narrow width of the f_0, so the zeros must be not so much far from the mass values.

Scalar and vector resonances

- The real term presents a zero close to the mass of the vector meson ρ and another one close to the mass of $f_0(980)$. There is also a change of signal of the CP violation associated to the $cos\theta$ passing through zero around the middle of the Dalitz plot.

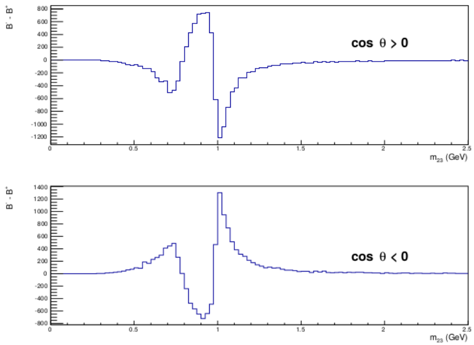

Figure 24: A simulation of CP violation for the $B^{\pm} \to K^{\pm}\pi^{+}\pi^{+}$ decay, with only contribution of the real part of Dalitz interference CP violation. The figure on the top corresponds to the events with $\cos\theta > 0$ while the bottom one $\cos\theta < 0$.

Scalar and vector resonances

- The imaginary term presents the peak of the two interfering resonances. Due to the directly proportionality to the $cos\theta$, there is a change of signal of the CP violation when $cos\theta$ pass through zero at the middle of the Dalitz plot.

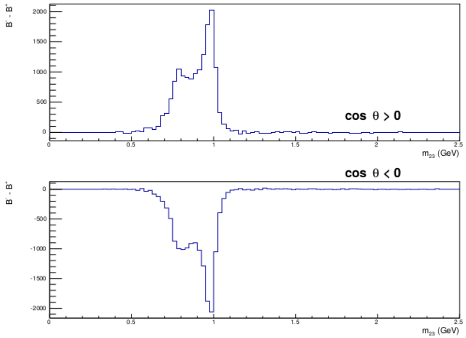

Figure 25: A simulation of CP violation for the $B^{\pm} \to K^{\pm}\pi^{+}\pi^{+}$ decay, with only contribution of the imaginary part of Dalitz interference CP violation. The figure on top corresponds to the events with $\cos\theta > 0$ while the bottom one $\cos\theta < 0$.